THE REVIEW OF PHYSICAL CHEMISTRY OF JAPAN, VOL. 50, 1980

HIGH PRESSURE LUMINESCENCE*

By H. G. Drickamer

In this review we discuss high pressure luminescence in liquids and polymer films to 10-12 kbar pressure, as well as studies in polymer films and crystalline solids to over 100 kbar. We use these results to characterize excitations and to test theories concerning radiative and non-radiative processes.

The organic systems discussed include:
(a) several polyenes where a theory relating the effective Stokes shift to the radiative rate is tested;
(b) several dyes in liquid solution where a theory relating viscosity to luminescence efficiency is tested;
(c) polymer films involving polyvinylcarbazole, where the two excimer states are characterized.

The inorganic systems include:
(a) ZnS with appropriate dopants, where a theory of the luminescence efficiency is tested;
(b) Europium doped oxysulfides where a model describing emission from the various excited states is tested.

1. Introduction

Over the past few years high pressure luminesence studies have proved to be very effective for characterizing electronic study and electronic processes in condensed systems. A number of factors have contributed to this development including photon counters for detecting very low light levels, and very intense light sources as well as sources and detection systems permitting measurements on time scales faster than a nanosecond, and sophisticated methods for transforming and analyzing data to extract lineshapes, intensities, and lifetimes.

In this review it is my intention to present a few selected examples to illustrate applications to organic molecules, in liquid and polymeric solutions and to inorganic crystalline solids.

For localized excitations many of the features are illustrated effectively in terms of a configuration coordinate diagram (Fig. 1). The configuration coordinate can be any normal mode of motion of the system, but pressure generally couples most strongly to the totally symmetric (breathing) motion which is simply related to the volume. For molecular systems one will primarily be concerned with an intermoleclar coordinate. The ground and first

(*Received June 9, 1980*)

*This work was supported in part by the U. S. Department of Energy under Contract DE-AC02-76-ERO1198.

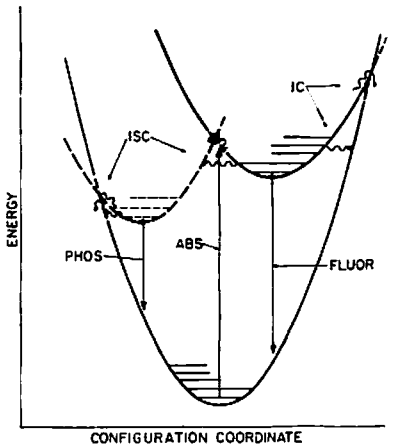

Fig. 1. Schematic configuration coordinate diagram.

allowed excited electronic states are represented by potential wells (in first order, harmonic). These will, in general, have different displacements along the coordinate and possibly different force constants. Optical absorptions and emissions are vertical (Franck-Condon) processes. The horizontal lines represent vibrational sublevels of the electronic states. An excited electron may emit vibrational energy until it reaches the bottom of the (excited state) well and fluoresce. Alternatively, it may return thermally to the ground state (internal conversion, (IC)); classically, by surmounting the energy barrier, or quantum mechanically through overlap of vibrational wave functions. The relative rates of the optical and thermal processes determine, in first order, the fluorescence efficiency.

On the other hand, the electron may cross over by a similar radiationless process to an optically forbidden (*e. g.* a triplet) state. This intersystem crossing (ISC) can also quench fluorescence. From the triplet state, it may phosphoresce, or return thermally to the ground state. Since phosphorescence is generally slow, $10^{-6}-10^{6}$ seconds, only for heavy atoms where spin-orbit coupling is large is there significant phosphorescence at room temperature.

The simplest effect of pressure is to displace the potential wells with respect to one another, vertically and/or horizontally.[1] The first order effect of this displacement is to change the rates of the radiationless processes and thus to modify the quantum efficiency. It is also possible to perturb the shape of the potential wells. For a pure harmonic oscillator the force constant is independent of volume, but there is always some anharmonicity present. In principle, one can include anharmonic terms, but it is difficult to obtain sufficient data for accurate evaluation and anharmonic coupling terms make the normal mode analysis less valid. In any case, the single configuration coordinate model is best adapted for qualitative or simple first order quantitative treatment of data.

A simple conclusion from Fig. 1 is that generally a decrease in the energy difference between the first excited state and the ground state should result in an increase in the rate of intersystem crossing and a decrease in phosphor efficiency and that an increase in the

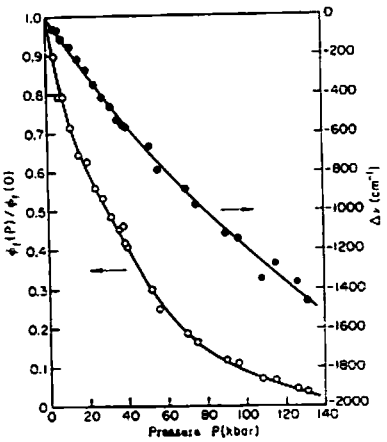

Fig. 2a. Peak shift and intensity change with pressure--$S_2 \rightarrow S_0$ transition for azulene derivative in PMMA (polymethyl methacrylate).

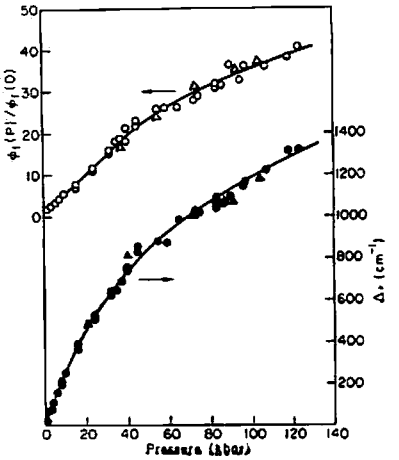

Fig. 2b. Peak shift and intensity change with pressure--$S_1 \rightarrow S_0$ transition for azulene derivative in PMMA.

energy difference should have the inverse effect. This phenomenon is conveniently illustrated[2] by a study of an organic molecule (a derivative of azulene) in a rigid polymeric matrix. The system is selected because emission is observed from two excited states, one (S_2) distinctly more polarizable than the ground state, and the other (S_1) less polarizable than the ground state. As can be seen from Fig. 2a and 2b, the emission from S_2 shifts to lower energy by $\sim$1500 cm^{-1} ($\sim$0.2 eV) in 100 kbar and the efficiency drops by a factor of fifty; on the other hand, the emission from S_1 increases in energy by about 0.2 eV in 100 kbar and the efficiency increases by a factor of $\sim$40-50.

2. Polyenes

The linear conjugated polyenes have been widely studied as prototypes for molecules of biological significance. We discuss here the effect of pressure on the radiative rate parameters for fluorescence for 1,6-diphenyl-1, 3, 5-hexatriene (DPH) and 1, 8-diphenyl-octaterane (DPO) in liquid solution. We mention also studies of these molecules plus retinyl acetate in polymer films.

Hudson and co-workers[3,4] have shown that for many polyenes the positions of 0-0 absorption and fluorescence bands in solution are given by an expression of the form:

$$\nu = \nu_0 - \alpha L, \qquad (1)$$

where ν_0 is the energy of the transition in the gas phase, α is the solvent polarizability, $(n^2-1)/(n^2+2)$, n is the solvent index of refraction, and L is a constant related to the oscillator strength of the transition. The strong absorption occurs in solution 2000-3000 cm^{-1} to the red

of its gas phase position giving a value of L of about 10^4 cm^{-1} per unit change in α. Values of L obtained from plots of fluorescence frequency *vs.* α are typically a factor of 5-20 smaller.[3] Therefore as α is increased, the energy gap ΔE between the allowed $^*B_u(S_2)$ and forbidden $^*A_g(S_1)$ state rapidly decreases. Since this gap is only 1000-2000 cm^{-1} in the lower polyenes, a significant perturbation can be introduced by fairly small changes in α.

Andrews and Hudson[5] have used a perturbation theory approach to derive an expression for the solvent dependence of the radiative rate of a forbidden transition in the presence of vibronic mixing. Their expression has the form

$$k_f=\frac{9n^3}{(n^2+2)^2}\frac{\Gamma^2}{(\Delta E^2)}, \tag{2}$$

where Γ is constant for a given molecule and ΔE is the energy difference between the lowest vibrational level of the emitting A_g excited state and a value obtained from a weighted integration of the B_u absorption spectrum over its vibronic levels. As mentioned above, ΔE is a strong function of solvent α so that Eq. (2) predicts a radiative rate which is very sensitive to solvent polarizability. Analysis of radiative rate data for DPH and *trans*-retinol in several solvents and over a large temperature range gave quantitative agreement with theory.

Birks and co-workers[6,7] have used a similar expression

$$k_f=\frac{k_{f2}V^2}{(\Delta E_{0-0})^2}=\frac{n^2k_{f20}V^2}{(\Delta E_{0-0})^2} \tag{3}$$

to describe the solvent and temperature effect on the $S_1\rightarrow S_0$ radiative rate k_f in DPH and DPO. In this expression ΔE_{0-0} is the energy difference between the 0-0 bands of absorption and emission and V is the matrix element coupling the $S_1\rightarrow S_0$ and $S_2\rightarrow S_0$ transitions. k_{f2} is the $S_2\rightarrow S_0$ radiative rate in cyclohexane obtained from the experimental absorption spectrum *via* the Birks-Dyson relation.[8] $k_{f20}(=k_{f2}/n^2)$ has been observed to be independent of solvent and temperature for many organic solutes in several solvents.[9] Plots of k_f *vs.* $(n/\Delta E_{0-0})^2$ were found to be linear giving V values of 745 cm^{-1} for DPH and 500 cm^{-1} for DPO.

The peak positions obtained by computer fitting of a skewed Gaussian curve to the

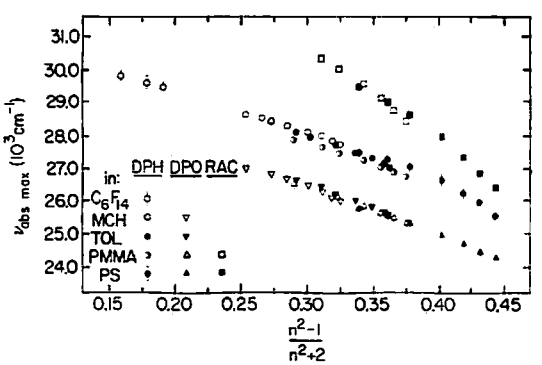

Fig. 3. Plot of energy of absorption centroid *vs.* solvent α for DPH, DPO, and RAc in various media.

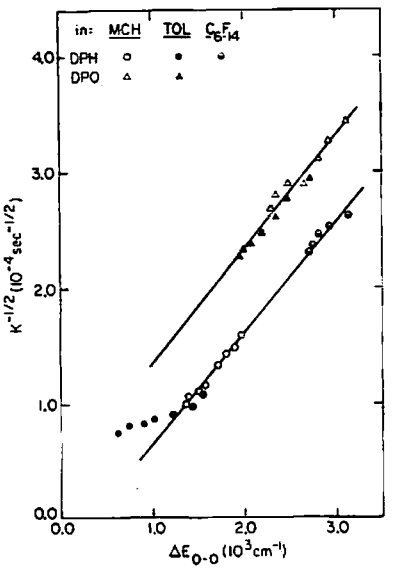

Fig. 4. $K^{-1/2}$ *vs.* ΔE in fluid solution (see text for definition of terms).

corrected excitation spectra are plotted *vs.* solvent α in Fig. 3. The plots are fairly linear (correlation coefficient >0.99) in accordance with Eq. (1). Slopes are 14600 for DPH and DPO, and 29300 for RAc. These compare to slopes of 10600 for DPH[4] and 10909 for octateraene[10] from solvent and temperature variation studies. A slope of about 6500 for RAc can be obtained from data in Ref. (4). The reason for the very large pressure induced shifts in RAc is unknown.

The value of C as determined from the center of the area under the excitation spectrum appeared to be the same for a given compound in any medium. so in Fig. 4 we plot $k^{-1/2}$ *vs.* ΔE_{0-0}. Figure 4 shows data for DPH and DPO in the liquid cell all to 10 kbar except for DPH in C_6F_{14} (which freezes above 1.5 kbar). Over much of the experimental range, the data exhibit the linear dependence on ΔE_{0-0} predicted by Eq. (3). For DPH in toluene the data points for which $\Delta E_{0-0}<1000$ cm^{-1} were disregarded in determining the linear fits shown. As ΔE_{0-0} becomes small (<1000 cm^{-1}) the simple first order intensity borrowing expression begins to fail. This is to be expected as the experimental radiative rate approaches the rate calculated from the $B_u \leftarrow A_g$ absorption intensities. Γ values calculated from the data are 1.0×10^7 cm^{-1} $sec^{-1/2}$ for both DPH and DPO. This compares to a value of 0.8×10^7 cm^{-1} $sec^{-1/2}$ for DPH given in Ref. (5).

The studies in polymeric media to 40 kbar also gave linear fits for plots like Fig. 4. for DPO and DPH with values of Γ equal to 6×10^6 and 1.2×10^7 cm^{-1} $sec^{-1/2}$, respectively. For retinyl acetate the model fails. possibly because there are $n\pi^*$ states lying between the $^*B_u$ state to which the allowed absorption takes place and the $^*A_g$ state from which the emission occurs.

3. Viscosity Effects on Luminescence Efficiency

Another example of the use of high pressure concerns the viscosity dependent quenching of the fluorescence of the triphenylmethane dye crystal violet (CV) and the diphenylmethane dye auramine O(AO) in alcoholic solution.

Studies of viscosity dependent processes in fluid media are usually carried out by varying the composition or the temperature of the solvent. The problem then arises of separating the viscosity dependence from purely temperature and/or solvent effects. The use of pressure allows a significant range of viscosities to be attained in a single solvent at a single temperature. If a wider range of viscosities is desired, chemically similar solvents for which the attainable viscosities overlap can be utilized. In this way very large viscosity range can be investigated at one temperature with only a few solvents.

In this example[12] pressures to 11 kbar were used on methanol, *iso*-propanol, *iso*-butanol, and glycerol to obtain solvent viscosities from less than 10^{-2} poise to more than 10^{+3} poise at room temperature. The solute concentrations were in the range $2\text{-}4\times10^{-6}$ M.

Forster and Hoffman (FH)[13] have investigated the fluorescence efficiency of several triphenylmethane dyes including CV in a variety of solvents at different temperatures. FH propose a model to explain the observed dependence of ϕ on η in which the dye molecule is excited to a Franck-Condon vertical state with the phenyl rings still at the ground state equilibrium angle θ_o. The rings then rotate towards a new equilibrium angle θ_o' at a rate controlled by Stokes-like viscous damping. $(\theta-\theta_o')$ therefore decreases exponentially with a relaxation time proportional to η. The non-radiative viscosity dependent deactivation rate of the excited singlet is taken to be proportional to $(\theta-\theta_o)^2$. There is also a non-radiative viscosity independent deactivation which accounts for the limiting value of ϕ in highly viscous media. In solvents of very low viscosity, the model predicts a viscosity independent minimum value for ϕ. This limiting case was not observed.

The data for CV are shown in log-log form in Fig. 5. The AO data has been displaced along the arbitrary intensity axis to show that for log $\eta > \sim 0.5$ the two dyes exhibit identical

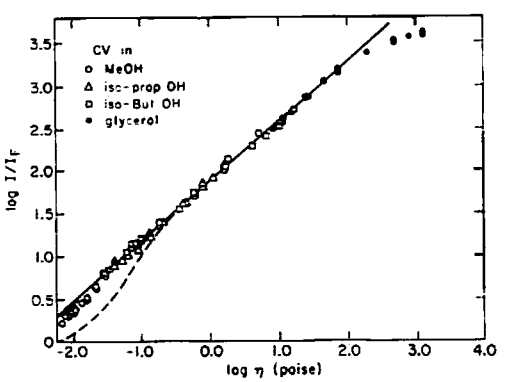

Fig. 5. Log luminescence efficiency *vs.* log viscosity (η).

dependence of fluorescence efficiency on solvent viscosity. The dashed line in Fig. 5 indicates the deviation of the AO intensities at low η. The line of slope 0.7 drawn in Fig. 5 shows excellent agreement with the CV data over 3.5 orders of magnitude in viscosity. At very low η there is a small but definite deviation from linearity and at high η the intensities begin to level off. The AO data is also linear with a slope of 0.7 over a smaller range of 2.5 orders of magnitude in viscosity. It exhibits identical limiting behavior at high η, but much larger deviations from linearity at low η. It should be noted that the deviation at low viscosity is towards a *larger* viscosity dependence of the fluorescence intensity. The FH theory predicts a leveling. *i.e.*, a lower viscosity dependence at low viscosities. We do not at present have an explanation for this discrepancy.

4. Excitations in Polymers

Polyvinylcarbazole is a polymer of much theoretical and practical interest and its optical properties have been widely studied. An important feature of the emission spectrum is the presence of two emission peaks assigned to two different excimer emissions in the regions 22.5-23.5 kK and 25-26 kK.

In this study[14] different films of PVCA in dilute solution with another polymer and a film of pure PVCA were subjected to pressures up to 40 kbar, and changes in the emission characteristics with pressure were observed and recorded. The data included peak location, the total emission intensity as well as the relative integrated intensity of each excimer emission, and the lifetime of such excimer as a function of pressure. The peaks shifted significantly to lower energy with pressure. The total intensity behaves similarly for PVCA in PMMA and in PS, as well as for the PVCA film. There is an initial small increase in intensity, followed by a decrease at higher pressures. The only differences are in the magnitude of the increase, and in the pressure at which the maximum occurs. The behavior of PVCA in PIB is similar at high pressures, but there is an initial decrease, followed by a rapid increase initiating at about 5 kbars, which is not present in the other films.

The ratio of I_{D_2}/I_{D_1} was calculated and is shown in Figs. 6 and 7, for the low and high pressure regions respectively. The semilogarithmic plots show two regions where the data are reasonably linear. At low pressures there is a steeper slope for all four films, which changes to a less steep one as the pressure is raised above a certain point. The transition between regions is not sharp and occurs approximately at 2 kbar for pure PVCA, 4 kbar for PVCA in PS, 6 bar for PVCA in PMMA, and 14 kbar for PVCA in PIB. The two slopes indicate the existence of two mechanisms; one controlling at the "low" pressure region and the other at the "high" pressure region. The lifetimes mirrored roughly the intensity changes, especially at high pressure, which indicates that there was no significant effect of pressure on radiative rates. At all but the lowest pressure the ratio of lifetimes from the two excimer emissions was essentially independent of pressure.

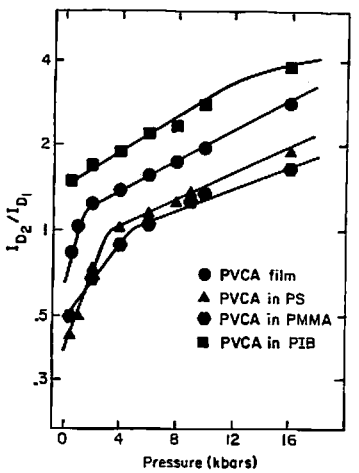

Fig. 6. Ratio of emission intensities I_{D_2}/I_{D_1} *vs.* pressure—low pressure region for polyvinylcarbazole excimers.

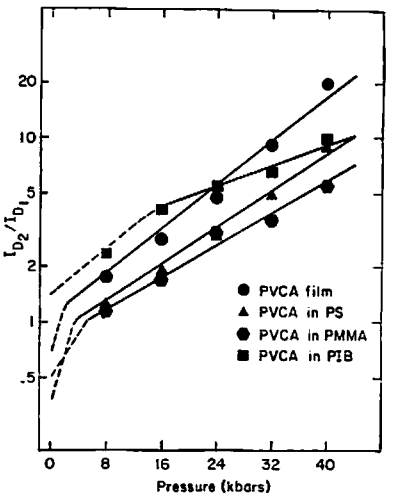

Fig. 7. Ratio of emisson intensities I_{D_2}/I_{D_1} for polyvinylcarbazole excimers.

It is clear from the presentation of the results that two distinct mechanisms of excimer interaction are involved. One is evident at high pressures, and the other is present only at low pressures. The pressure at which the transtion from one to the other occurs is solvent dependent. An explanation of the emission behavior of PVCA can be provided, using the kinetic scheme of Fig. 8 with some appropriate simplifications and assumptions. The nomenclature is an extension to that used by Birks,[15] and the mechanism is similar to that described by Johnson.[16] The rate constants k_{FM} and k_{IM} are those for radiative and non-radiative deactivation of the excited monomer respectively, with k_{FD_1}, k_{FD_2} and k_{ID_1}, k_{ID_2}

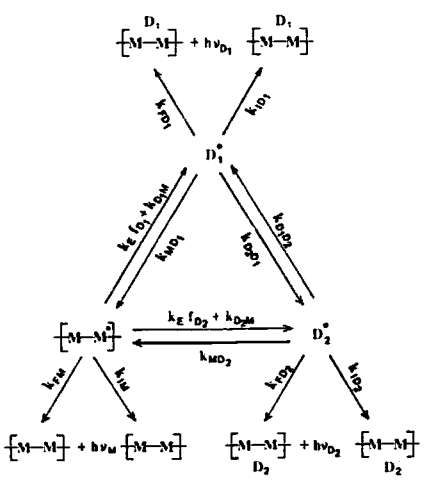

Fig. 8. Scheme of reactions—polyvinylcarbazole.

having the corresponding for the two excimers. D_1 and D_2 represent the excimers responsible for the 380 nm and 430 nm bands respectively. The star (*) represents an excited singlet state: unlike Johnson's nomenclature, D_1 and D_2 refer to ground state potential excimer sites and not the excited complexes, $k_{D_1D_2}$ and $k_{D_2D_1}$ are the association and dissociation rates of D_1 and D_2, with k_{D_1M}, k_{MD_1} and k_{D_2M}, k_{MD_2} representing the same quanties between the monomer and the two excimers. The mechanism, represented by the last four rate constants, involves main chain conformational changes and/or side group motion to achieve the geometrical requirements necessary for excimer formation during the lifetime of excitation. $k_Ef_{D_1}$ and $k_Ef_{D_2}$ correspond to singlet exciton migration to preformed sites along the polymer chain, which satisfy the requirements for excimer formation prior to excitation; k_E represents the rate of energy transfer of singlet excitons and f_{D_1}, f_{D_2} are the concentrations of preformed excimer sites. This mechanism applies to both solutions and solid films of PVCA, but some of the rate constants become insignificant in films, depending on the temperature and pressure.

Eq. (4) is slightly modified from Johnson's Eq. (6):

$$\frac{I_{D_2}}{I_{D_1}} = \frac{k_{FD_2}}{k_{FD_1}} \frac{k_{D_2D_1}(f_{D_2}+f_{D_1})+k_{D_1}k_{D_2}}{k_{D_1D}(f_{D_2}+f_{D_1})+k_{D_2}f_{D_1}}. \tag{4}$$

In our case, f_{D_2} and f_{D_1} include the probability of capture of an exciton by a D_2 or D_1 site: they are therefore effective concentrations. In order to simplify Eq. (2), one can consider the following limiting cases:

(a) $k_{D_1D_2} \ll k_{D_2}$, $k_{D_2D_1} \ll k_{D_1}$ (*i. e.* no rotations are allowed to any appreciable extent), and Eq. (2) becomes

$$\frac{I_{D_2}}{I_{D_1}} = \frac{k_{FD_2}\tau_2 f_{D_2}}{k_{FD_1}\tau_1 f_{D_1}}, \tag{5}$$

where $\tau_1 = 1/k_{D_1}$, $\tau_2 = 1/k_{D_2}$.

If the ratio of radiative rates and the ratio of lifetimes are not varying, I_{D_2}/I_{D_1} depends only on the change of the relative probability of capture of an exciton by a D_2 or D_1 site.

(b) $k_{D_1D_2} \gg k_{D_2}$, $k_{D_2D_1} \gg k_{D_1}$ (*i. e.* a rearrangement between D_1 and D_2 is allowed, and proceeds efficiently). In this case Eq. (2) becomes

$$\frac{I_{D_2}}{I_{D_1}} = \frac{k_{FD_2}}{k_{FD_1}} \frac{k_{D_2D_1}}{k_{D\,D_2}}. \tag{6}$$

If the ratio of the radiative rates does not change, I_{D_2}/I_{D_1} depends on the rotational equilibrium constant between D_1 and D_2.

Any intermediate cases, where one of $k_{D_2D_1}$ is negligible relative to the other, cannot occur in a plastic medium, because it would deplete the respective population and resulting emission from of one the sites: this follows because there is no other way of forimng or depleting sites.

In order to distinguish between mechanisms, it is useful to know the glass transition

Table 1. Glass transition temperatures of polymer films

Polymer	T_g(K)	Reference
PVCA	423	[17]
	481	[18]
	498	[19]
PS	373	[20-21]
PMMA (isotactic)	318	[22-23]
	328	[24]
PIB	200	[18, 25]

temperatures (T_g) of the different polymer films, and these are shown in Table 1. On a molecular scale, the glass transition temperature is the temperature above which the polymer has acquired sufficient thermal energy for rotational motion, or considerable torsional oscillation, to occur about the majority of bonds in the main chain. Below this temperature, this form of motion takes place infrequently and the majority of inchain groups have fixed conformations. Some transitions can still occur at $T<T_g$: Boyer[22] has classified those and proposed that they be called $T_{g'}$.

If such a transition is taking place between D_2 and D_1 at atmospheric pressure, one would eventually expect it to stop at some higher pressure, which should corollate inversely with T_g. In other words, the higher T_g, the lower the pressure, at room temperature, that the transition between D_2 and D_1 should stop. This, in fact, is observed with our data if we assume that the $D_2 \leftrightarrow D_1$ transition is the controlling factor at low pressures. From Figs. 6 and 7 it is evident that the pressures at which the change in slope occurs have the following order:

$$P(\text{PVCA in PIB}) > P(\text{PVCA in PMMA}) > P(\text{PVCA in PS}) > P(\text{PCVA film}).$$

Also from Table 1:

$$T_g(\text{PIB}) < T_g(\text{PMMA}) < T_g(\text{PS}) < T_g(\text{PVCA}).$$

This correlation leads one to conclude that mechanism (b) dominates at low pressures, and only mechanism (a) is present at high pressures. We can now examine each pressure region separately.

(a) At the high pressure region, τ_2/τ_1 is approximately constant.[14] The radiative rates (k_{FD_i}) are also constant with pressure. One can then take the logarithm of both sides of Eq. (5) to get

$$\ln\frac{I_{D_2}}{I_{D_1}} = \text{Constant} + \ln\frac{f_{D_2}}{f_{D_1}}. \qquad (7)$$

The number of preformed excimer sites cannot be changing, since all pathways of forming or destroying them do not exist at high pressures. What must be changing is the relative probability of capture. At equilibrium, this can be represented by a constant k_c, which is related to known thermodynamic quantities by

$$k_c \propto e^{-(\Delta G_c/RT)}, \tag{8}$$

and

$$\frac{\partial \ln(k_c)}{\partial P} = \frac{\partial \ln(I_{D_2}/I_{D_1})}{\partial P} = -\frac{\Delta V_c}{RT}, \tag{9}$$

where ΔG_c is the change of the Gibbs free energy for the above process. The volume extracted from this treatment is a thermodynamic equilibrium quantity, and represents the difference in volume of the system between the $D_1 \rightarrow D_1^*$ and $D_2 \rightarrow D_2^*$ transitions. This process can be expected to extend to the low pressure region also, but its contribution is small relative to process (b) (see Fig. 7), and to a first approximation it can be subtracted out.

(b) In the low pressure region k_{FD_2}/k_{FD_1} is also approximately constant, and taking the logarithm of both sides of Eg. (4) gives

$$\ln \frac{I_{D_2}}{I_{D_1}} \simeq \text{Constant} + \ln \frac{k_{D_2D_1}}{k_{D_1D_2}}. \tag{10}$$

A change in the relative intensities is then only dependent on the change of the equilibrium distribution of the two sites. Similarly

$$\frac{k_{D_2D_1}}{k_{D_1D_2}} \propto e^{-(\Delta G_{12}/RT)}, \tag{11}$$

and

$$\frac{\partial \ln(k_{D_2D_1}/k_{D_1D_2})}{\partial P} = -\frac{\partial \ln(I_{D_2}/I_{D_1})}{\partial P} = -\frac{\Delta V_{12}}{RT}. \tag{12}$$

ΔV_{12} represents the change in volume of the system for $D_1^* \rightarrow D_2^*$.

One can extract these volumes from the slopes of the different lines in Figs. 6 and 7. The approximate molar volume (V_{mol}) can also be calculated from the density (1.509 g/cm^3).[38] and the molecular weight (193.2 g/mole) of the monomer: V_{mol}=182.4 cm^3/mole. ΔV's and ΔV's/V_{mol} of PVCA in all polymer films are given in Table 2.

The first observation one can make is that there is a net reduction of the system volume for both processes. ΔV_{12}, which represents the process of $D_2^* \rightarrow D_2^*$, is at its largest only 3% of total molar volume, which indicates that a very small rearrangement is necessary to achieve this. This confirms that the initial assumption of some movement in the polymer films is

Table 2. ΔV's of PVCA in all host polymers

Polymer	ΔV_c(cm^3/mole)	$\Delta V_c/V_{mol}$	ΔV_{12}(cm^3/mole)	$\Delta V_{12}/V_{mol}$
PVCA film	−2.0	0.011	−5.1	0.028
PVCA in PS	−1.6	0.009	−5.0	0.027
PVCA in PMMA	−1.1	0.006	−3.9	0.021
PVCA in PIB	−0.9	0.005	−2.1	0.013

possible at low pressures. A second observation is that the change in volume for the two processes is solvent dependent. The order of decreasing T_g is followed by the decreasing ΔV's, which implies that the less rigid solvents can rearrange with less volume change.

The observations of the total intensity variation with pressure also confirm the assumptions made about the nature of the controlling mechanisms. Emission of the D_2 excimer is efficient ($\tau_2 > \tau_1$). and any shift of the equilibrium distribution towards D_2 can be expected to increase the total intensity. The extent and pressure range where the increase occurs, follows the same order as that of the existence of mechanism (b). The largest increase in intensity is observed for PVCA in PIB for which equilibrium between D_1 and D_2 is affected by pressure over the largest range. The smallest increase in intensity is observed for the PVCA film, for which mechanism (b) is in effect over the shortest range of pressure. The eventual decrease in intensity can be attributed to an increase of the non-radiative rate (k_{1D}) with pressure. This is due to the fact that radiationless transitions to the ground state increase as the separation of the two states decreases. From the above argument one would expect the order of quenching by internal conversion to be:

$$Q(\text{PVCA film}) > Q(\text{PVCA in PS}) > Q(\text{PVCA in PMMA}) \gg Q(\text{PVCA in PIB}),$$

and this is experimentally observed.

5. Zincblende Emission

Crystals have the zincblende-like structure, with appropriate dopants, are utilized commercially in television screens, light emitting diodes and a variety of other applications.

We present here a study of ZnS as a prototype[25] although similar results are obtained for related systems. Figure 9 presents a schematic outline of the principle electronic states and excitations. The basic excitation is from the top of the valence band to the bottom of the conduction band. Two types of dopants are added (in concentrations $\sim$0.01 atom %). A Cu^+ or Ag^+ ion acts as a hole trap. It is a deep trap, 1-1.5 eV above the valence band, and thus is strongly localized. There is a variety of evidence[26] that its position vis-a-vis the top of the

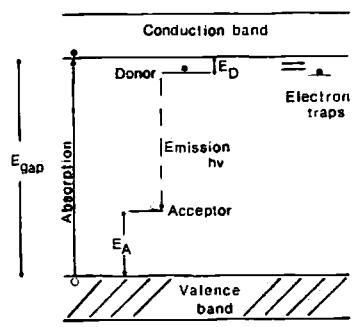

Fig. 9. Schematic diagram of band structure and impurity levels—ZnS doped with donors and acceptors.

valence band is quite independent of pressure. A second compensating ion (*e.g.* Cl^-, Al^{+3}) acts as an electron trap with a trap depth E_D of ~0.1-0.2 eV. This trap depth is sensitive to conditions, and the delocalization of the electron trap weve function is stronly dependent on E_D. The luminescence efficiency depends directly on the overlap and thus on the delocalization of E_D. The relevant equation for the intensity[26,27] can be written:

$$I(r) \propto \frac{1}{\tau} \int r^2 W(r) G(r) \, dr, \tag{13}$$

where $W(r)$, the radiative recombination rate, is given by

$$W(r) = \text{const} \times (r/a^*)^{2(N-1)} \exp(-2r/Na^*). \tag{14}$$

Here

$$N = \frac{E^{*1/2}}{E_D}, \quad E^* = \frac{e^2}{2a^*\varepsilon}, \quad a^* = \frac{h^2\varepsilon}{m^* e^2}.$$

m^* is the effective electronic mass and ε is the dielectric constant. The distribution function $G(r)$ used corresponded to a random distribution of impurities.

The major pressure dependence of the intensity arises through N and thus through E_D. We use here two independent ways of measuring E_D as a function of pressure. First, we measure the shift of the absorption edge and of the emission peak with pressure and take the difference of these as the change in E_D with pressure. It is assumed that the hole trap energy E_A is independent of pressure. There are several pieces of evidence[25] that this is a reasonable assumption, but establishing a small number from the difference between two large numbers always involves an element of risk. We later check the measurement of E_D by a second method.[28] Figure 10 shows the shift of the absorption edge and the luminescence emission

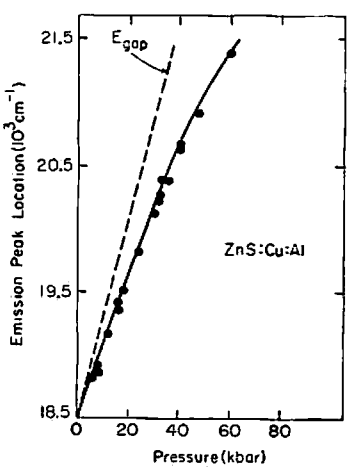

Fig. 10. Shift of absorption edge and of luminescence emission peak with pressure—doped ZnS.

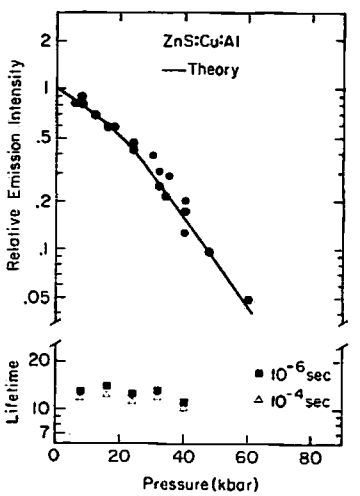

Fig. 11. Comparison of relative values calculated and measured luminescence efficiency—doped ZnS.

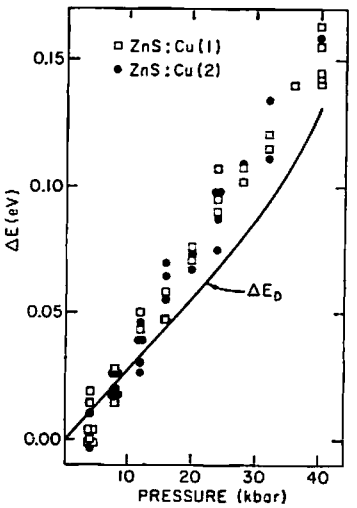

Fig. 12. Comparison of E_D (donor trap depth) *vs.* pressure from thermoluminescence and from steady state measurements.

with pressure. It is clear that E_D increases significantly as pressure increases. In Fig. 11 we compare the relative efficiency as caculated from Eq. (13) with the measured values. The agreement is remarkably good. (In the lower part of the figure are shown two lifetimes which are essentially independent of pressure. The complex decay was approximated as a double exponential. The independence of pressure is consistent with our assumption that E_A is pressure independent).

In spite of the satisfactory comparison of theory with experiment, it is desirable to check the pressure effect on E_D by a second method.[28] If the sample of ZnS is irradiated at say 77 K, no emission is observed. Heating the sample after irradiation generates an emission which maximizes at some temperature T_m. Of the heating is performed so that the temperature-time curve is linear, it is straightforward to extract E_D, from the heating rate and T_m. In Fig. 12 values of the change in E_D with pressure from thermoluminescence data are compared with the value from the steady state measurements[25] discussed earlier. The discrepancy is nowhere greater than 0.01 eV which is surely within the error of the experiments and of the theory. It is encouraging that rather different heating rates generated the value for E_D.

These results illustrate rather well the ability of pressure to test a model of a material of both theoretical and practical interest.

6. Eu^{+3} in Oxysulfides

A second type of useful solid state phoshor involves an oxysulfide doped with Eu^{+3}. Here we discuss primarily La_2O_2S: Eu, with a few remarks about Y_2O_2S: Eu. These materials are used in fluorescent lighting and as prototypes for lasers.

The excitation lies in the ultraviolet at about 4-4.2 eV, and involves a partial charge transfer from sulfur to europium. The excitation is transferred to excited ^5D level of Eu^{+3}

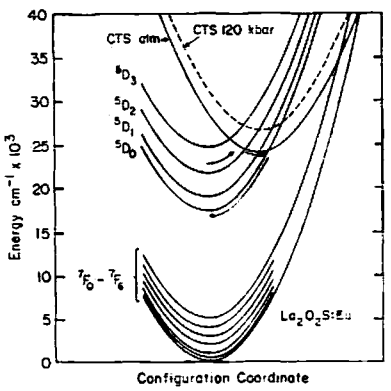

Fig. 13. Schematic configuration coordinate diagram. La_2O_2S : Eu.

which are split by spin-orbit coupling into the series $^5D_0$, $^5D_2$, and $^5D_3$ in order of increasing energy. Since this levels be from 1.9 to 2.9 eV above the ground state one would expect to observe emission from all four levels. In the lanthanum salt only $^5D_0$ and $^5D_1$ emit at room temperature, with a weak $^5D_2$ emission at very low temperature. Struck and Fonger[30] have proposed a solution for this anomaly based on the observed temperature coefficient of emission intensity : their proposal is illustrated in the configuration coordinate diagram of Fig. 13. The charge transfer (CT) state does indeed feed all the ^5D levels of Eu^{+3}, but the radiative lifetime of the ^5D levels in long and the energy barrier to backfeeding into the CT state very low so the latter process governs. Backfeeding from $^5D_2$ also occurs with a slightly smaller efficiency, so that emission is observed at one atmosphere only from $^5D_1$ and $^5D_0$.

If we consider the CC diagram of Struck and Fonger to represent a slice along the totally symmetric coordinate, then pressure experiments should provide a test of this model: since the CT state lies at a larger value of the configuration coordinate, it should shift energy with pressure and thus affect the backfeeding from $^5D_3$ and $^5D_2$ to the CT state. Such high pressure experiments have been performed. As can be seen from Fig. 14, the CT state does indeed shift to higher energy with pressure by over 0.25 eV (2000 cm^{-1}) in 100 kbar. The effect on the emission from the ^5D levels is summarized in Fig. 15. The emission

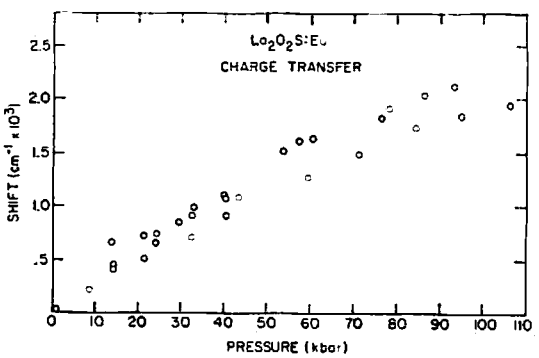

Fig. 14. Shift of CT (charge transfer) state with pressure—La_2O_2S : Eu.

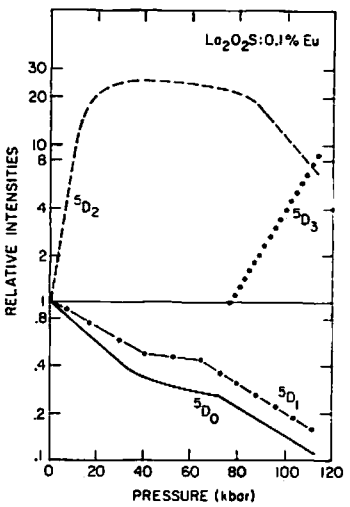

Fig. 15. Emission intensity *vs.* pressure—^5D levels of Eu^{+3} in La_2O_2S.

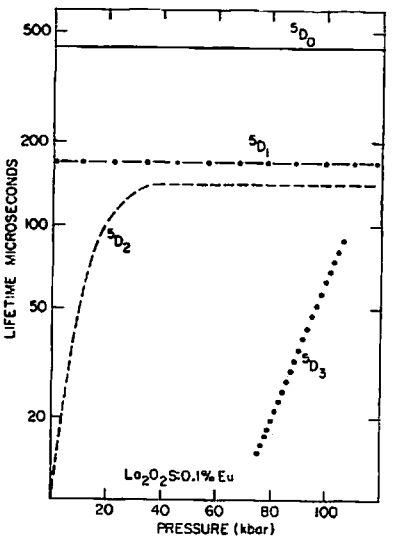

Fig. 16. Lifetimes *vs.* pressure—^5D levels of Eu^{+3} in La_2O_2S.

from $^5D_0$ and $^5D_1$ decreases as pressure increases, with a small but definite leveling at intermediate pressures. The $^5D_2$ emission increases rapidly for ~40 kbar levels, and there drops beyond ~ 90 kbar. The $^5D_3$ emission appears with sufficient intensity for quantiative measurement at 70–75 kbar and increases rapidly in intensity at higher pressures. As far as we could estimate, the total intensity of emission from all ^5D levels is essentially independent of pressure. The effect of pressure on the lifetimes is exhibited in Fig. 16. The $^5D_0$ and $^5D_1$ lifetimes are pressure independent since only the feeding is affected. The $^5D_2$ lifetime increases when the intensity increases and then levels. The $^5D_3$ lifetime increases rapidly with pressure as would be expected.

From the shift of the CT peak one can calculate the increase in the energy barrier for backfeeding with pressure. If we add this number to the atmospheric pressure estimate of Struck and Fonger we can predict the increase in intensity of emission from $^5D_2$ and $^5D_3$ with pressure using a simple classical model. In Fig. 17 we compare prediction and measurement; the agreement is quite satisfactory.

The yttrium salt exhibits qualitatively similar behavior to the lanthanium, except that the CT peak initially lies at about 1000 cm^{-1} (0.125 eV) higher energy for the Y_2O_2S: Eu. The situation at one atmosphere corresponds roughly to that for La_2O_2S: Eu at ~50 kbar. Indeed there is significant $^5D_2$ emission at room temperature. Its intensity decreases with increasing pressure, at first slowly and then more rapidly. The $^5D_3$ emission appears at ~ 25 kbar in contrast to La_2O_2S: Eu where it appears near 75 kbar. It increases rapidly in intensity with pressure. In Fig. 18 exhibit the comparison between calculation and experiment obtained by the same technique discussed for Fig. 17 above. Agreement is, again, excellent.

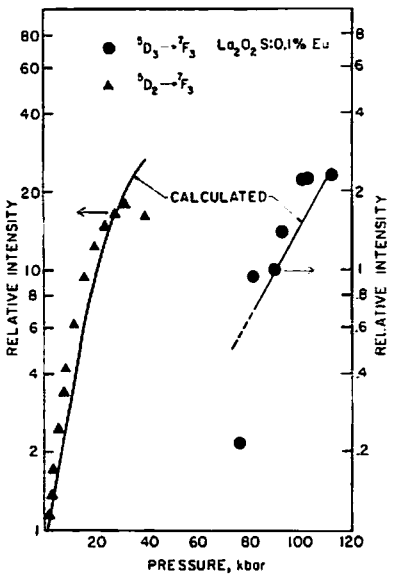

Fig. 17. Calculated and measured emisson intensity *vs.* pressure La_2O_2S: Eu ($^5D_2$ and $^5D_3$ levels of Eu).

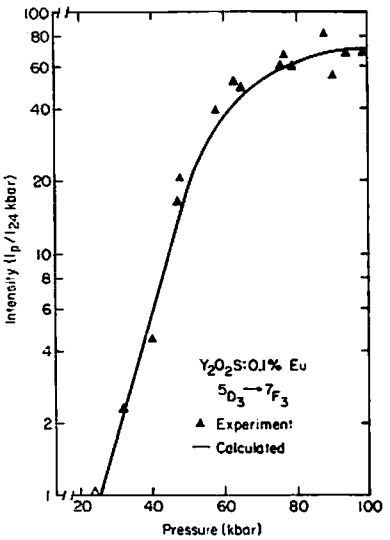

Fig. 18. Calculated and measured emission intensities *vs.* pressure Y_2O_2S: Eu ($^5D_3$ level of Eu).

It should be mentioned that all of the above discussion applies to dilute (~0.1% Eu) materials. Above about 0.5-1.0% Eu significant concentration quenching effects occur. The reader is referred to the original paper for a discussion of how concentration quenching affects the pressure data.

While the results presented here constitute only a small fraction of the variety of studies we have made, they illustrate both the breadth and power of high pressure as a tool for understanding luminescence in particular and electronic structure in general.

References

1) H. G. Drickamer, C. P. Slichter, and C. W. Frank, *Proc. Nat. Acad. Sci.*, 69, 933 (1972).
2) D. J. Mitchell, H. G. Drickamer, and G. B. Schuster, *J. Am. Chem. Soc.*, 99, 7489 (1977).
3) B. S. Hudson and B. Kohler, *Chem. Phys. Lett.*, 14, 299 (1972); *J. Chem. Phys.*, 59, 4984 (1973).
4) L. A. Sklar, B. S. Hudson, W. Petersen, and J. Diamond, *Biochemistry*, 16, 813 (1977).
5) J. R. Andrews and B. S. Hudson, *J. Chem. Phys.*, 68, 4587 (1978).
6) J. B. Birks and D. J. S. Birch, *Chem. Phys. Lett.*, 31, 608 (1975).
7) J. B. Birks, G. N. R. Tripathi, and M. D. Lumb, *Chem. Phys.*, 33, 185 (1978).
8) J. B. Birks and D. J. Dyson, *Proc. R. Soc. Ser.*, A275, 135 (1963).
9) R. B. Cundall and L. C. Pereira, *J. Chem. Soc. Faraday Trans. II*, 68, 1152 (1972).
10) R. W. Gavin, C. Weisman, J. D. McVey, and S. A. Rice, *J. Chem. Phys.*, 68, 522 (1978).
11) J. Mallik, K. M. Jain, K. Mandal, and T. N. Misra, *Ind. J. Pure Appl. Phys.*, 13, 699 (1975).
12) L. A. Brey, G. B. Schuster, and H. G. Drickamer, *J. Chem. Phys.*, 67, 2648 (1977).
13) T. H. Förster and G. Hoffman, *Z. Physik. Chem., N. F.*, 75, 63 (1971).
14) G. Chryssomallis and H. G. Drickamer, *J. Chem. Phys.*, 71, 4817 (1979).
15) J. B. Birks, "Photophysics of Aromatic Molecules", Wiley-Interscience, London (1970), Chap 7.
16) G. E. Johnson, *J. Chem. Phys.*, 62, 4697 (1975).

17) A. Willbourn, *Trans. Faraday Soc.*, 54, 717 (1958).
18) L. E. Nielsen, "Mechanical Properties of Polymers", Reinhold (1962).
19) Private communication with Dr. J. Pochan.
20) R. Wiley and G. Bauer, *J. Polymer Sci.*, 3, 455 (1948).
21) R. Beevers and E. White, *J. Polymer Sci.*, B1, 171 (1963).
22) R. Boyer, *Rubber Chem. Technol.*, 36, 1303 (1963).
23) G. Martin, S. Rogers, and L. Mandelkern, *J. Polymer Sci.*, 20, 579 (1956).
24) G. Schulz, W. Wunderlich, and R. Kirste, *Macromol. Chem.*, 75, 23 (1964).
25) G. L. House and H. G. Drickamer, *J. Chem. Phys.*, 67, 3221, 3227, 3230 (1977).
26) J. S. Prener and F. E. Williams, *J. Chem. Phys.*, 25, 361 (1956).
27) D. G. Thomas, J. J. Hobfield, and W. M. Augustiniak, *Phys. Rev.*, A140, 202 (1965).
28) J. W. Hook, III and H. G. Drickamer, *J. Appl. Phys.*, 49, 2503 (1978).
29) W. H. Fonger and C. W. Struck, *J. Chem. Phys.*, 52, 6364 (1970).
30) G. A. Webster and H. G. Drickamer, *J. Chem. Phys.*, 72, 3740 (1980).

School of Chemical Sciences
and
Materials Research Laboratory
University of Illinois at Urbana-Champaign
Urbana, Illinois 61801
U. S. A.